

Citation: Retscher, C., G. Kirchengast, and A. Gobiet, Ozone and Temperature Retrieval Results from GOMOS Validated with CHAMP and ECMWF, in *Atmosphere and Climate: Studies by Occultation Methods* (U. Foelsche, G. Kirchengast, A.K. Steiner, eds.), pp. 55-66, Springer, Berlin-Heidelberg, 2006.

Ozone and Temperature Retrieval Results from GOMOS Validated with CHAMP and ECMWF

C. Retscher, G. Kirchengast, and A. Gobiet

Wegener Center for Climate and Global Change (WegCenter) and Institute for Geophysics, Astrophysics, and Meteorology (IGAM), University of Graz, Austria
christian.retscher@uni-graz.at

Abstract. Data from the Global Ozone Monitoring by Occultation of Stars (GOMOS) instrument on-board the European environmental satellite Envisat have been used for retrieval of ozone and temperature profiles by new algorithms, followed by profile validation. We discuss ozone profiles, determined from GOMOS transmission data, validated with operational GOMOS ozone profiles and ECMWF (European Centre for Medium-Range Weather Forecasts) analysis data. For ozone we developed an optimal estimation retrieval scheme, using sensibly selected channels from the Spectrometer A transmission spectra within 260 nm to 340 nm and 602 nm to 634 nm. Furthermore, profiles of a new GOMOS temperature profile retrieval are compared to CHAMP (CHALLENGING Minisatellite Payload) and ECMWF analysis data. GOMOS temperatures are gained by exploiting pointing data of the Steering Front Assembly (SFA) and the Star Acquisition and Tracking Unit (SATU), which provide information on the refraction of the star light in the atmosphere and thus allow to derive refractive bending angle profiles. The bending angle profiles are then converted via refractivity and pressure profiles to temperature profiles. Bending angles were assumed to have errors of $3 \mu\text{rad}$. Statistical optimization of observed bending angles with model bending angles was used to provide adequate data quality for the Abel transform from the stratopause region upwards, which led to a significant gain in temperature retrieval accuracy up to 40 km height due to suppressed downward propagation of errors induced by Abel transform and hydrostatic integral. Based on data from year 2002, a set of GOMOS ozone and bending angle derived temperature profiles is validated and discussed.

1 Introduction

The Global Ozone Monitoring by Occultation of Stars (GOMOS) (Bertaux et al. 1991; Kyrölä et al. 1993; Kyrölä et al. 2004) sensor on-board Envisat is a self-calibrating instrument intended to provide data on the trace gas ozone, and chemicals favoring its depletion such as NO_2 , NO_3 , BrO , and ClO . Atmospheric reference profiles are measured under dark and bright

limb conditions obtaining very good global coverage with about 300 high-quality profiles per day and a height resolution of about 1.5 km. GOMOS records the transmission of radiation passing the atmosphere along a path from the star to the instrument. Its Spectrometer A measures ozone and ozone depleting chemicals within a wavelength range from 250 nm to 675 nm and provides a spectral resolution of 1.2 nm.

GOMOS star tracking and acquisition (SFA/SATU) data is exploited for obtaining bending angles of rays passing the atmosphere. These bending angles, highlighting the effect of atmospheric refraction, allow to derive atmospheric refractivity profiles and subsequently temperature profiles.

We present and discuss ozone and retrieved temperature profiles based on an analysis of year 2002 data. The algorithm is based on temperature dependent cross-section data of the corresponding GOMOS database, standard climatological atmospheric profiles for the trace gases, and CIRA model profiles for background temperature and pressure.

2 GOMOS Retrieval Schemes

2.1 Ozone Retrieval

The spectrometer A on the GOMOS instrument provides transmission data from 250 nm to 375 nm and 405 nm to 675 nm at a spectral sampling of ~ 0.3 nm. In the method presented here only a few available channels were selected by empirical arguments and tests on the algorithm. The selected channels were chosen to give a good signal response in the Hartley and Huggins band and as well in the Chappuis band, which is especially important for lower stratosphere ozone retrieval. The set of wavelengths selected for presentation in this work contains 14 channels with $\lambda \in [260, 280, 288, 295, 302, 309, 317, 328, 334, 337, 340, 343, 600, 605]$, where numbers are given in [nm]. A more rigorous analysis including information content theory is postponed for future enhancements of the retrieval scheme (cf., Sofieva and Kyrölä 2004; Sofieva and Kyrölä 2003).

The atmospheric transmission is defined by Beer-Bouguer-Lambert's law at each wavelength λ of interest, by incorporating ozone, NO_2 , NO_3 , and bulk air background information. This forward model is a best estimate of the current atmospheric state. Due to a currently low stratospheric aerosol concentration a term representing the corresponding signal extinction – the Mie scattering – was neglected, but we plan to integrate it in next steps of algorithm enhancements.

Having a forward model established, we have to find an inverse connection between measurements (transmission data) and targeted state (ozone profile) of the atmosphere. In the case presented here, ozone and NO_2 are retrieved simultaneously, forming a joint retrieval. The enhancement of the inversion

scheme by incorporating other trace gases (e.g., NO_3 , BrO , and OClO) targeted in the operational GOMOS retrieval is possible, but not investigated here. The measured transmission contains information of the density of the absorbing species and of the atmospheric refraction. To proceed from the transmission function one can find a solution for, e.g., the ozone density, by first separating the absorbing species by a spectral inversion and then perform a vertical inversion via an Abel transform. This is known as the two-step retrieval and is realized in the GOMOS operational processing (Paulsen 2000). Performing such a retrieval includes several restrictions one has to be aware of. Due to a line-by-line vertical retrieval, a correlation of adjacent vertical lines is not given any more after a following spectral inversion. This is not observed in nature, where depending on altitude and selected wavelength the bending of rays and thus the absorption of light by target species has a vertical correlation. This feature can be handled by a one-step inversion first performing a vertical retrieval (Vanhellemont et al. 2004). In the case of GOMOS this would include an inversion of large matrices (containing all wavelengths), which is then time consuming but can be processed in a proper way.

Here we use a different approach for the inversion of atmospheric species densities. Discrete inverse theory as discussed in detail by Rodgers (1976, 1990, 2000) provides a framework, where the forward model can be seen as an algebraic mapping of the state space into the measurement space. The physics of the measurement is approximated by the forward model and we introduce an operator \mathbf{K} , which here will be the Jacobian matrix (weighting function matrix) with the dimension $m \times n$ for m measurements and n elements of the state vector. The forward model reads $\mathbf{y} = \mathbf{K}\mathbf{x} + \boldsymbol{\varepsilon}$. Because of this generally non-linear equation, it is obvious that a straightforward solution for \mathbf{x} by direct inversion is not feasible. The direct inverse mapping would be $\mathbf{x}_r = \mathbf{K}^{-g}\mathbf{y}$, where \mathbf{K}^{-g} denotes a general inverse matrix and \mathbf{x}_r is the retrieved state. As the problem of interest here is ill-posed at high altitudes due to low signal-to-noise ratio (it may also be over-determined if we use more measurements than unknown states; $m > n$), we cannot directly employ the latter but rather constrain the solution by incorporating sensible *a priori* information. The Bayesian approach is the method of choice to solve such inverse problems perturbed by noise, where we have rough but reliable prior knowledge of the behavior of a state of interest. If the problem is only moderately non-linear we can use a Gauss-Newton method for an iterative approach to find an optimal solution. Assuming Gaussian probability distributions and a linearized forward model, the primary task of a retrieval method is to find a state by satisfying optimal criteria from an ensemble of states, which best agree with the *a priori* state and with the measurement within experimental errors.

Here we make use of a fast converging iterative optimal estimation algorithm,

$$\mathbf{x}_{i+1} = \mathbf{x}_{\text{ap}} + \left(\mathbf{K}_i^T \mathbf{S}_\varepsilon^{-1} \mathbf{K}_i + \mathbf{S}_{\text{ap}}^{-1} \right)^{-1} \mathbf{K}_i^T \mathbf{S}_\varepsilon^{-1} \left[(\mathbf{y} - \mathbf{y}_i) + \mathbf{K}_i (\mathbf{x}_i - \mathbf{x}_{\text{ap}}) \right], \quad (1)$$

where \mathbf{x}_{i+1} is the retrieved, \mathbf{x}_{ap} the *a priori* profile, \mathbf{y} the measurement vector, and $\mathbf{y}_i = \mathbf{K}_i \mathbf{x}_i$ the forward-modeled measurement vector. Key ingredients of Eq. 1 are the *a priori* covariance matrix \mathbf{S}_{ap} and the measurement error covariance matrix \mathbf{S}_ε . Diagonal elements of \mathbf{S}_{ap} for ozone are assumed to have 30 % standard deviation, while off-diagonal elements follow an exponential drop-off with a correlation length of 6 km. NO₂ variances have values of 40 % and covariances are set equally to ozone. The Jacobian (weighting) matrix \mathbf{K}_i represents the mapping involved. Index i is the iteration index, which is started by using $\mathbf{x}_0 = \mathbf{x}_{\text{ap}}$.

The number of needed iteration steps for Eq. 1 is found by a calculation of the cost function

$$\chi_i^2 = (\mathbf{y} - \mathbf{y}_i)^T \mathbf{S}_\varepsilon^{-1} (\mathbf{y} - \mathbf{y}_i) + (\mathbf{x}_i - \mathbf{x}_{\text{ap}})^T \mathbf{S}_{\text{ap}}^{-1} (\mathbf{x}_i - \mathbf{x}_{\text{ap}}) \quad (2)$$

at each iteration step i . The cost function χ_{i+1}^2 at iteration step $i+1$ has always to be smaller than χ_i^2 . The minimum criterion is met if χ_i^2 is smaller than the number of selected channels. If this criterion is not reached the retrieval stops per definition after 10 iterations.

2.2 Temperature Retrieval

The GOMOS temperature retrieval follows a different method compared to the ozone retrieval procedure. Instead of introducing a third matrix, besides ozone and NO₂, for a joint retrieval, temperature profiles are inverted by an Abel transform. Light coming from, e.g., stellar sources undergo a refractive bending before the signal gets measured by the instrument. The degree of refraction is a measure for the atmospheric density, pressure, and temperature, respectively.

GOMOS derived bending angles have their origin in an exploitation of the elevation movement of the star tracking unit (SFA/SATU) (cf., Sofieva et al. 2003). The star image is kept inside the CCD with a sampling of 100 Hz and errors of $\pm 10 \mu\text{rad}$ from the central position. The measured elevation angles are compared to an unrefracted ray, measured outside the atmosphere and thus giving a bending angle profile.

For the derivation of refractivity profiles from bending angles and impact parameters using the Abel transform, we assume local spherical symmetric conditions. A correction for the ellipsoidal shape of the Earth is applied.

In theory one can now start with the calculation of the refractive index, which is the next step in the temperature retrieval procedure. If the bending angle $\alpha(a)$ is given, we find for the Abel transform

$$n(r_0) = \exp \left[\frac{1}{\pi} \int_{\alpha=\alpha(a_0)}^{\alpha=0} \ln \left(\frac{a(\alpha)}{a_0} + \sqrt{\left(\frac{a(\alpha)}{a_0} \right)^2 - 1} \right) d\alpha \right], \quad (3)$$

written here in a favorable form for numerical use by avoiding poles (cf., Steiner 1998; Foelsche 1999). The refractive index is denoted by n and $\alpha(a_0)$

is the bending angle dependent on the impact parameter a_0 , associated with radius r_0 , the bottom height of the Abelian integration, which extends over the height domain above r_0 . From n follow density, pressure, and temperature profiles by applying the hydrostatic equation and the ideal gas law.

Bending angles at high altitudes, due to small refraction, are typically very small numbers with large error bars. Measurement errors and errors of discretization further decrease the quality of bending angle profiles. The signal-to-noise ratio in the measured bending angle profile becomes less than unity at altitudes above ~ 40 km. Due to the application of the Abelian integral and the hydrostatic equation, errors in the bending angle profile at high altitudes propagate down through all height steps and thus also low altitude temperature profiles suffer from an inappropriate initialization value as explained, e.g., by Syndergaard (1999). A sensible use of good-quality bending angle data for high-altitude initialization is therefore needed and realized by the introduction of the statistical optimization technique.

The statistical optimization (Sokolovsky and Hunt 1996) optimally combines measured and background (*a priori*) bending angle profiles leading to the most probable bending angle profile. An optimal solution can be found via

$$\alpha_{\text{opt}} = \alpha_{\text{b}} + \mathbf{B}(\mathbf{B} + \mathbf{O})^{-1}(\alpha_{\text{o}} - \alpha_{\text{b}}), \quad (4)$$

where α_{b} is the background and α_{o} the observed bending angle profile, respectively. The matrices \mathbf{B} and \mathbf{O} express the background and the observation error covariances, respectively, which are found similar to \mathbf{S}_{ap} and \mathbf{S}_{ε} . The correlation length L was set to 6 km for \mathbf{B} , while we found $L = 1$ km appropriate for \mathbf{O} . As a background profile we chose a CIRA-86 climatology (e.g., Rees 1988). Background errors were assumed to be 20% in line with radio occultation literature (e.g., Healy 2001; Gobiet and Kirchengast 2002). The observation errors were estimated from the root-mean-square deviation of the observed data from the background at high altitudes (70 km to 80 km), where noise dominates the measured signal. More details on the statistical optimization scheme used here are found in, e.g., Gobiet and Kirchengast (2002, 2004); Retscher (2004); Gobiet et al. (2005).

In radio occultation, due to the selected wavelengths in the order of centimeter to meter, an ionospheric correction (e.g., Syndergaard 2000) is necessary and thus is an important issue. Rays in the optical, UV, and NIR wavelength range are not affected by the ionosphere and thus such a correction is not an issue.

3 Retrieval Results

For the retrieval of ozone profiles we used level 1b and level 2 data from the official GOMOS data product in the validation periods in September 2002,

20 – 27, October 2002, 11 – 13, and December 2002, 02. Both data products were processed and provided by ACRI-ST (Sophia Antipolis, France). The level 2 data were used as validation reference. Here we reduced the set of available data by eliminating those with large errors in level 1b transmissions and reference level 2 ozone data (cf., Retscher 2004). Measured transmissions were smoothed by running means and then corrected for scintillation and refractive dilution effects (cf., Paulsen 2000), which has a significant positive impact on the lower stratospheric ozone retrieval quality. ECMWF T511L60 analysis data (60 height levels, spherical harmonics truncation 511) were taken for the same period, where GOMOS data were available.

The quality of transmission data is further strongly dependent on the star magnitude, the star temperature, and the obliquity of the occultation. Light coming from bright stars is able to penetrate the Earth’s atmosphere down to lower heights than light stemming from weak stars. In general the penetration depth of light into the atmosphere is known to be wavelength dependent. In our analysis we found an ozone retrieval dependence mostly on the star temperature. Stars with temperatures between 8 000 K and 11 000 K clearly favor the retrieval as there the corresponding maximum of the Planck function lies within the UV wavelength range. This is reflected by a large number (passing the quality check) of contributing profiles in the error statistics of stars like Sirius (-1.44^m , 11 000 K), Fomalhaut (1.16^m , 9 700 K) and δ Velorum (1.95^m , 10 600 K).

Here we present the statistics of globally distributed occultation events separated by date and latitude regimes. The latitude regimes are divided into low ($0^\circ - 30^\circ$), mid ($30^\circ - 60^\circ$), and high ($60^\circ - 90^\circ$) latitudes. Such a selection is especially useful for looking at ozone trends in the high latitude profiles, where the ozone density is significantly diminished. Large scale stratospheric ozone depletion is mostly reported from high latitudes, where meteorological conditions favor depletion processes.

Figure 1 presents ozone validation results. The graphs include data of occultations of stars between -1.44^m and 3.03^m . Stars with magnitudes greater than 3.03^m show significantly larger errors and are not considered. We applied a quality check, by not considering profiles with errors larger than 50% (compared to official GOMOS level 2 data) between altitudes of 30 km and 60 km.

We found good retrieval performance in all latitude regions, where biases against level 2 data are found $\sim 5\%$ from 25 km to 65 km. Below 25 km – the lower altitude boundary of the measurements – we encounter a tendency to large biases. Above 65 km most profiles tend to negative biases with values of 20% at 70 km. This reflects the fact that data measured at such altitudes have small transmission values and large fluctuations, which affects the retrieval quality. In general, differences between the operational retrieval and the retrieval discussed here may have reasons in the selected wavelength region, as well as in the retrieval method itself, by retrieving only two species at once (NO_2 is retrieved simultaneously to support the ozone retrieval quality,

but it is not considered as a retrieval product in the current version of the application) instead of performing a full inversion of measured data. Future enhancements of the code will deal more properly with these effects.

Errors from the ECMWF validation show a clear bias of about -30% . This bias is known to be in the ECMWF product (cf., e.g., Dethof 2004; Bracher et al. 2004). Ozone is fully integrated into the ECMWF forecast model and analysis system as an additional three-dimensional model and analysis variable similar to humidity. The forecast model includes a prognostic equation for the ozone mass mixing ratio with a parameterization of sources and sinks of ozone.

A profile validation with ECMWF can be useful, if the observed biases behave almost equally throughout our profile validation. Validation at high latitudes has a bias, with values mostly between -20% and -30% , while the validation with mid latitudes has large positive deviations. The low latitude profile validation performs similar to the high latitude, but with larger positive biases below 25 km.

In the temperature retrieval simulation we have shown the influence of bending angle optimization on corresponding temperatures. We discuss the results of our real GOMOS SFA/SATU data temperature retrieval (cf., Retscher et al. 2004). Statistically optimized bending angles from GOMOS SFA/SATU data lead to temperature profiles and are then compared to ECMWF analyses and WegCenter retrieval results based on CHAMP profiles (cf., Gobiet et al. 2004). For this analysis, the GeoForschungsZentrum (GFZ) in Potsdam provided CHAMP data.

As already found for the ozone retrieval, the results of a GOMOS temperature retrieval strongly depends on the selected star and its magnitude as well as on its corresponding temperature. In general, one finds for bending angles and temperatures that a low star magnitude, favorably below 0, allows for retrievals into the troposphere down to heights of around 5 km, which is the theoretical minimum of GOMOS occultation data.

In our selected set of data, bending angles were available for the same period as given for ozone. The GOMOS occultation events cover different latitude regions, but especially in the high altitude region there is clear need for more occultation data. The GOMOS level 1b data product is separated into three latitude regions as done for ozone. A global set of retrieved data is given, where dependences on different latitude regions of the quality of an overall profile can be seen. GOMOS SFA/SATU (level 1b) data in general suffers from different influences. SFA/SATU data often show much larger errors than we estimated, by considering $10\ \mu\text{rad}$ at 100 Hz (in our application $3\ \mu\text{rad}$ at 10 Hz). The data set, which was provided for this study, only includes a small set of occulter stars, which makes it especially difficult to ensure good retrieval quality at high latitudes.

For this work we first validated GOMOS temperature profiles with CHAMP data. Phase delays from the CHAMP level 2 (version 2) (cf., Wickert et al. 2004) data served as input into our retrieval, which had ECMWF data as background information (cf., Gobiet et al. 2004). From 3724 CHAMP profiles

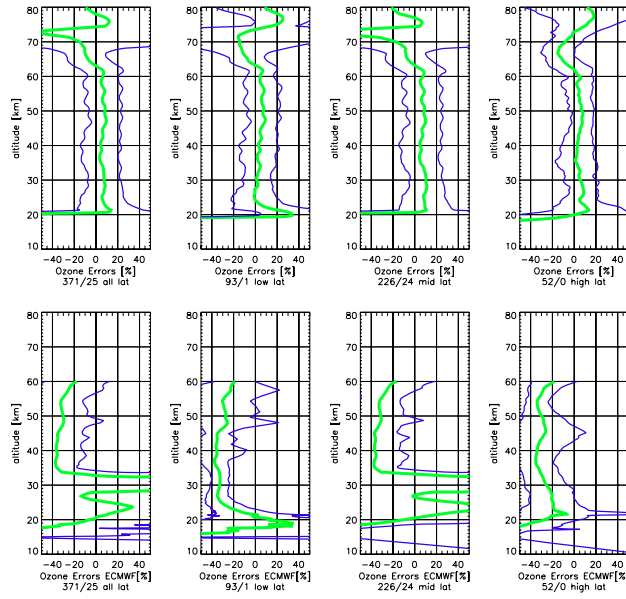


Fig. 1. Ozone error statistics for multi day ensembles in the period 2002-09-20 – 2002-12-02 (whole set 2002). In the upper panels we present results from ensembles validated with GOMOS level 2 (operational product) files and in the lower panels we validate with ECMWF analysis data. From the left, the first panel shows the overall statistics, the second, third, and fourth panel show the low, mid, and high latitude selected statistics. The heavy gray line denotes the bias profile $\hat{\mathbf{b}}$, while the enveloping fine black lines are the bias \pm standard deviation profile $\hat{\mathbf{b}} \pm \hat{\mathbf{s}}$. To each error profile contributes a certain number of available retrieved profiles passing the quality check. This is given below each plot, where on the left one finds the number of accepted profiles and the right number denotes the outliers (e.g., upper left: 371 accepted, 25 rejected profiles).

we found 56 profiles, where our coincidence intervals (300 km/3 hrs) with GOMOS data were reached.

In Fig. 2 GOMOS level 1b data is validated with CHAMP data at altitudes between 20 km and 35 km. The high latitude bias profile $\hat{\mathbf{b}}$ is shifted to positive values for altitudes below 25 km, while the standard deviation is <5 K. This is due to the fact that only a small set of GOMOS data with very few selected stars for occultation was available. For altitudes higher than 25 km a negative bias of up to 2 K was found. At mid and high latitudes $\hat{\mathbf{b}}$ has a negative deviation below 25 km and performs similar to the high latitude sample. The global ensemble clearly averages over negative and positive drifts below 25 km and a positive tendency in $\hat{\mathbf{b}}$ can be seen.

For the comparison of GOMOS SFA/SATU data to ECMWF data we chose co-located vertically distributed temperatures and refractivity profiles

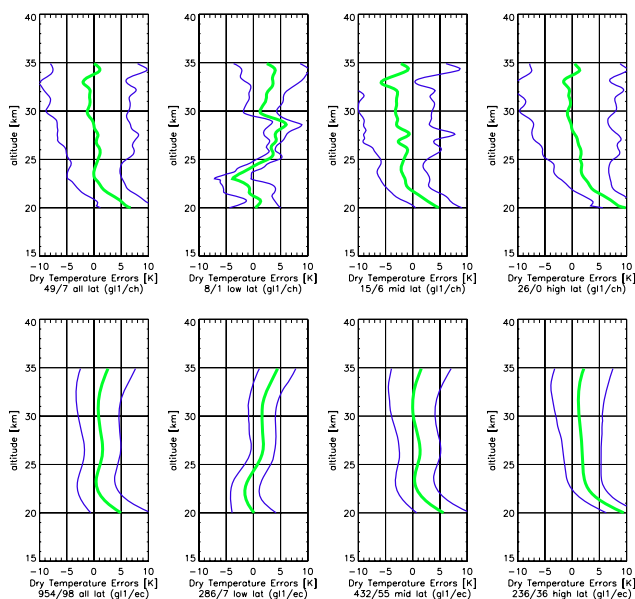


Fig. 2. Temperature error statistics for multi day ensembles in the period 2002-09-20 to 2002-12-02 (whole set 2002). In the upper panels we present results from ensembles validated with CHAMP GPS profiles and in the lower panels we validate with ECMWF analysis data. For further description of the graphs see caption of Fig. 1.

from the nearest analysis time of 6-hourly ECMWF T511L60 operational analysis data. ECMWF validation shows better results compared to the GOMOS-CHAMP validation. Typical features, as the positive bias for the low latitude profiles at altitudes >25 km are seen in the CHAMP and the ECMWF validation. At high latitudes and altitudes between 20 km and 35 km one can see the deviation to positive values of $\hat{\mathbf{b}}$. Due to interpolations, the profiles here appear more smoothed than in the GOMOS – CHAMP validation. For altitudes higher than 25 km a negative bias of >2 K was found. At mid and high latitudes $\hat{\mathbf{b}}$ has a positive deviation below 25 km and performs equally to the high latitude sample.

The validation results with ECMWF have smaller biases than the validation with CHAMP profiles. This has different reasons. First, the validation set with CHAMP profiles, especially at low and mid latitudes is too small, so that the bias profile suffers from errors at few single profile validation results (cf., Retscher 2004). A second reason is that coincidence intervals between GOMOS and CHAMP data are often too large, while for ECMWF we first select analysis data at the exact tangent point location of GOMOS.

4 Summary and Conclusions

We developed an optimal estimation algorithm for retrieval of atmospheric trace gas profiles from Envisat/GOMOS-measured transmission data. In this study ozone profiles were retrieved, which is the primary focus of the algorithm, though the whole processing chain is capable of retrieving other trace gases simultaneously.

Furthermore, we applied refractive occultation retrieval to bending angle data from GOMOS star tracker data (SFA/SATU), gaining refractivity and temperature profiles. A simultaneous exploitation of atmospheric transmission and bending angles was not yet performed in this study but will be introduced as a future enhancement. This enhancement will allow to simultaneously retrieve ozone and temperature profiles in the stratosphere as well as atmospheric refractivity and density, which can be used to improve the background fields required by the ray tracing. These improvements will further aid the ozone retrieval, given that the star tracker data are of adequate quality allowing $< 5 \mu\text{rad}$ bending angle accuracy.

In conclusion, the approach adopted for an efficient retrieval of ozone and temperature profiles has yielded satisfactory results. Data from later periods than year 2002 as well as Envisat/MIPAS ozone and temperature profiles will be analyzed and validated in future.

Acknowledgements. The authors gratefully acknowledge discussions with and support by U. Foelsche, M. Schwärz, C. Rehr, and J. Ramsauer (WegCenter, Univ. of Graz, Austria) as well as V. Sofieva and J. Tamminen (FMI, Helsinki, Finland). The European Space Agency is thanked for operating the Envisat satellite and for its related Announcement of Opportunity for free access to Envisat data. We are especially thankful to B. Theodore and G. Barrot (ACRI-ST, Sophia Antipolis, France) for providing reprocessed GOMOS data. Furthermore, we are grateful to J. Wickert and T. Schmidt (GFZ, Potsdam, Germany) for providing CHAMP occultation data. C.R. received financial support for the work from Envisat Project AO-620/Part-I funded by the Austrian Ministry for Traffic, Innovation, and Technology and carried out under contract with the Austrian Space Agency.

References

- Bertaux JL, Megie G, Widemann T, Chassefiere E, Pellinen R, Kyrölä E, Korpela S, Simon P (1991) Monitoring of ozone trend by stellar occultations: the GOMOS instrument. *Advances in Space Research* 11:237–242
- Bracher A, Eichmann K, von Savigny C, Weber M (2004) Ozone Distribution in the Arctic Winter/Spring 2002/2003 as Measured by GOMOS, MIPAS, and SCIAMACHY. In: *Envisat Symposium 2004*, Salzburg, Austria
- Dethof A (2004) Assimilation of ozone data in the ECMWF Integrated Forecast System. In: *SPARC 2004*, Victoria, Canada

- Foelsche U (1999) Tropospheric water vapor imaging by combination of ground-based and spaceborne GNSS sounding data. Tech rep, No 10/1999, IGAM, Univ of Graz, Austria
- Gobiet A, Kirchengast G (2002) Sensitivity of atmospheric profiles retrieved from GNSS occultation data to ionospheric residual and high-altitude initialization errors. Tech rep, ESA/ESTEC No 1/2002, IGAM, Univ of Graz, Austria
- Gobiet A, Kirchengast G (2004) Advancements of Global Navigation Satellite System Radio Occultation Retrieval in the Upper Stratosphere for Optimal Climate Monitoring Utility. *J Geophys Res* 109(D24110), doi:10.1029/2004JD005117
- Gobiet A, Steiner AK, Retscher C, Foelsche U, Kirchengast G (2004) Radio Occultation Data and Algorithms Validation Based on CHAMP/GPS Data. Tech rep, No 1/2004 IGAM, Univ of Graz, Austria
- Gobiet A, Kirchengast G, Wickert J, Retscher C, Wang D, Hauchecorne A (2005) Evaluation of Stratospheric Radio Occultation Retrieval Using Data from CHAMP, MIPAS, GOMOS and ECMWF Analysis Fields. In: Reigber C, Lühr H, Schwintzer P, Wickert J (eds) *Earth Observation with CHAMP: Results from Three Years in Orbit*. Springer, Berlin, pp 531–536
- Healy S (2001) Smoothing Radio Occultation Bending Angles Above 40 km. *Ann Geophys* 19:459
- Kyrölä E, Sihvola E, Kotivuori Y, Tikka M, Tuomi T, Haario H (1993) Inverse theory for occultation measurements. I - Spectral inversion. *J Geophys Res* 98(17):7367–7381
- Kyrölä E, Tamminen J, Leppelmeier GW, Sofieva V, Hassinen S, Bertaux JL, Hauchecorne A, Dalaudier F, Cot C, Korablev O, d Andon OF, Barrot G, Mangin A, Thodore B, Guirlet M, Etanchaud F, Snoeij P, Koopman R, Saavedra L, Fraisse R, Fussen D, Vanhellemont F (2004) GOMOS on Envisat: An overview. *Advances in Space Research* 33:1020–1028
- Paulsen T (2000) GOMOS Level 1b/2 Algorithm Description Document for Envisat Pre-Release. Tech rep, ESA Doc, PO-TN-ESA-GM-1019, ESA/ESTEC, Noordwijk, Netherlands
- Rees D (ed) (1988) *COSPAR International Reference Atmosphere: 1986, Part I: Thermosphere Models*, vol 8
- Retscher C (2004) Stratospheric Ozone and Temperature Sounding by the Envisat/GOMOS Stellar Occultation Sensor. Tech rep, No 23/2004, IGAM, Univ of Graz, Austria
- Retscher C, Kirchengast G, Gobiet A, Hauchecorne A (2004) Stratospheric Temperature and Ozone Sounding with Envisat/GOMOS Stellar Occultation. In: Kirchengast G, Foelsche U, Steiner AK (eds) *Occultations for Probing Atmosphere and Climate*. Springer, Berlin, pp 299–308
- Rodgers C (1976) Retrieval of Atmos. Temperature and Composition from Remote Measurements of Thermal Radiation. *Rev Geophys* 14:609–624
- Rodgers C (1990) Characterization and Error Analysis of Profiles Retrieved From Remote Sensing Measurements. *J Geophys Res* 95:5587–5595
- Rodgers C (2000) *Inverse Methods for Atmospheric Remote Sounding: Theory and Practice*. World Scientific, Singapore
- Sofieva VF, Kyrölä E (2003) Information approach to optimal selection of spectral channels. *Journal of Geophysical Research (Atmospheres)* 108(D16):15, doi: 10.1029/2002JD002980

- Sofieva VF, Kyrölä E (2004) Information Approach to Channel Selection for Stellar Occultation Measurements. In: Kirchengast G, Foelsche U, Steiner AK (eds) *Occultations for Probing Atmosphere and Climate*, Springer, Berlin, pp 309–318
- Sofieva VF, Kyrölä E, Ferraguto M, Team GC (2003) From Pointing Measurements in Stellar Occultation to Atmospheric Temperature, Pressure and Density Profiling: Simulations and First GOMOS Results. In: *Geoscience and Remote Sensing Symposium, IGARSS '03, Proceedings*, vol 5, pp 2990
- Sokolovsky S, Hunt D (1996) Statistical Optimization Approach for GPS/Met Data Inversions. In: *URSI GPS/Met Workshop*, Tucson, Arizona
- Steiner AK (1998) High Resolution Sounding of Key Climate Variables Using the Radio Occultation Technique. Tech rep, No 3/1998, IGAM, Univ of Graz, Austria
- Syndergaard S (1999) Retrieval Analysis and Methodologies in Atmospheric Limb Sounding Using GNSS Radio Occultation Technique. PhD thesis, Niels Bohr Inst for Astron, Physics and Geophysics, Univ of Copenhagen
- Syndergaard S (2000) On the Ionosphere Calibration in GPS Radio Occultation Measurements. *Radio Sci* 35:865–883
- Vanhellemont F, Fussen D, Bingen C (2004) Global One-step Inversion of Satellite Occultation Measurements: A Practical Method. *J Geophys Res* 109(D18):9306, doi:10.1029/2003JD004168
- Wickert J, Schmidt T, Beyerle G, König R, Reigber C, Jakowski N (2004) The radio occultation experiment aboard CHAMP: Operational data analysis and validation of vertical atmos. profiles. *J Meteorol Soc Jpn* 82:381–395